INVESTIGATION OF THE ELECTRICAL BREAKDOWN OF A PLASMA–COLD ELECTRODE GAP

G. Yu. Dautov, M. F. Zhukov, G. M. Mustafin, and A. N. Timoshevskii

Zhurnal Prikladnoi Mekhaniki i Tekhnicheskoi Fiziki, Vol. 10, No. 2, pp. 67–72, 1969

Breakdown of the arc plasma–cold electrode gap in a segmented-channel plasma generator has been experimentally investigated. It is shown that γ processes at the cathode do not play an important part. Expressions are obtained for the dependence of breakdown potential on current, gas flow rate, and the distance from the anode spot. The experimental data are interpreted and generalized in criterial form.

NOTATION

r, z, φ—cylindrical coordinates
δ—width of discharge gap
p—gas pressure in discharge gap
γ—second ionization coefficient
n_i, n_e—ion and electron densities
i—discharge current per unit length of channel
U^*—Voltage (breakdown potential)
U_i—voltage drop across discharge gap
E_z, E_r—electric field strength components
H_φ—magnetic field strength component
I, U—arc current and voltage
G—air flow rate through plasma generator
a—distance between electrodes
Q_z—heat losses on length z
T_{eff}—effective gas temperature in breakdown gap
ξ—arc column radius
r_1, R—radii of coaxial electrodes
e—electron charge
v_i, v_e—drift velocities of ions and electrons in direction of z-axis
D_i, D_e—diffusion coefficients of ions and electrons
b_i, b_e—mobilities of ions and electrons

1. In a number of plasma devices an important role is played by breakdown of the gas between the plasma and a cold electrode. Thus, for example, in plasma generators with a self-stabilized arc the gas between the positive column and the channel wall periodically breaks down (shunting) [1–4]. Shunting limits the length of the arc and the temperature of the heated gas and causes large-scale fluctuations of the parameters of the arc and the flow. Breakdown of the arc plasma-electrode gap also plays an important part in plasma engines, high-voltage circuit breakers, etc.

In [5] the Townsend theory was used to describe breakdown in a plasma generator with a self-stabilized arc, i.e., the arc plasma was treated as an ordinary metal electrode surrounded by heated gas. In [6] the column of an open arc was also treated as a heated metal electrode, and breakdown was described by means of a combination of the Townsend theory and streamer theory.

In the case of breakdown of the gas between a plasma and an electrode the plasma behaves like a conductive gas containing free electrons and ions. When the plasma serves as cathode, the γ processes that form the basis of the Townsend-Rogowski theory are no longer required for the development of an electron avalanche. If the plasma serves as anode, it will contain the large number of free ions necessary for the realization of γ processes at the cathode, i.e., in this case also there is no necessity for ion multiplication by means of developing electron avalanches. Thus, in relation to breakdown of the plasma-cold electrode gap the basic premises of the Townsend-Rogowski theory become meaningless. Moreover, photoionization of the gas in the breakdown gap takes place under the influence of the arc radiation, charged particles diffuse into the gap from the arc column, and photoprocesses controlled by the arc radiation develop at the surface of the metal electrode. These factors, disregarded by the Townsend-Rogowski theory,

must affect the breakdown mechanism. Thus, in our present state of knowledge, deeper understanding of the phenomenon of breakdown of the plasma-electrode gap and the further development of the theory depend primarily on the accumulation of experimental data.

2. In our experimental investigation of breakdown we used a plasma generator with a segmented channel (Fig. 1). The water-cooled copper electrodes 1, 3 and segments 2, insulated from each other and the electrodes, form the arc chamber of the plasma generator. The distance between electrodes a = const (21 cm). Air is supplied through tangential holes in the swirler ring. Between the arc plasma and the inner wall of the segment there is a layer of relatively low-temperature air with very low electrical conductivity. In the presence of a potential difference between the plasma and the segment a weak-current semi-self-maintained discharge develops in this layer [7]. At a certain critical value of the potential difference breakdown takes place and the semi-self-maintained discharge becomes an arc discharge. In the experiments the voltage on the segments, whose inside diameter and thickness were equal to 1 cm, was supplied by the single-pulse generator whose circuit diagram is shown in Fig. 1. A typical oscillogram of the voltage pulse at i = 0 is given in Fig. 2. The regulated rise time of this pulse was of the order of 10^{-5} sec. The maximum value of the pulse was so selected that breakdown took place on the sloping part of the pulse. In order to limit and measure the value of the current after breakdown a resistance R' (shunt Sh_2) was introduced into the circuit between the generator and the segment. A DÉSO-1 double-beam oscillograph was used to record oscillograms of the breakdown voltage and current.

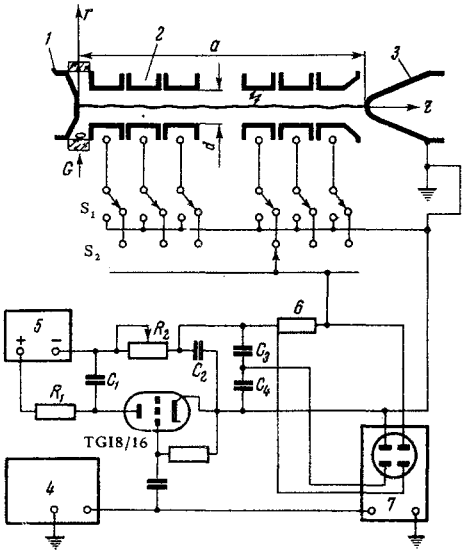

Fig. 1. Diagram of the experimental setup: 1) anode, 2) segments, 3) cathode; G—air supply, r, z—cylindrical coordinates.

The arc voltage and current were recorded by an M-366 voltmeter (class 1 accuracy) and an LM-1 instrument (class 0.5 accuracy), respectively.

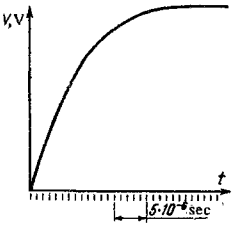

Fig. 2. Oscillogram of voltage pulse.

In the experiments I and U were varied in the ranges 80–160 A and 570–900 V, respectively.

3. Oscillograms of i, $U' = U_i + R_i'$ and U_i are presented in Fig. 3a, b for reverse polarity (plasma as anode,

segment as cathode). As can be seen from the oscillogram (Fig. 3a), the discharge current up to breakdown is very small, and U' varies with the open-circuit generator voltage. When $U' \approx U'_{max}$ breakdown occurs and i begins to increase rapidly, while U' decreases.

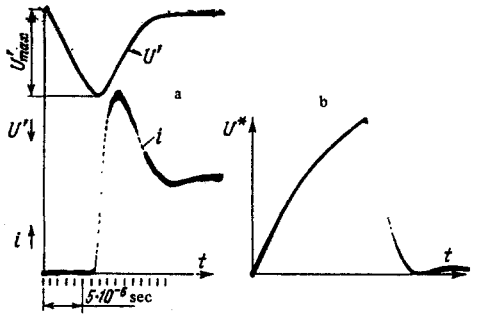

Fig. 3. Oscillograms of the discharge current and voltage: U = 910 V, I = 100 A, G = 8 g/sec, z = 10 cm, reverse polarity: a) R' = 3 ohm, b) R' = 0.

It is clear from Fig. 3b that after breakdown U_i decreases very sharply. The smoother decrease in U' in Fig. 3a immediately after breakdown is attributable to the rapid increase in i and hence iR'. However, before breakdown the values of i and iR' are small, and therefore it may be assumed that $U^* \approx U'_{max}$. In the case of normal polarity (plasma as cathode, segment as anode) the current increases more smoothly during breakdown and discharge development (Fig. 4). However, the discharge current before breakdown is also small and iR' is much less than U_i. Therefore, here again, it is possible to assume that $U^* \approx U'_{max}$.

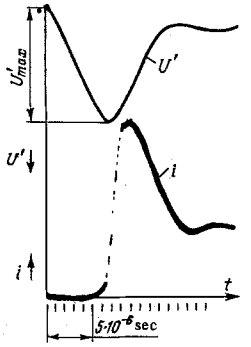

Fig. 4. Oscillograms of discharge current and voltage: U = 900 V, I = 100 A, G = 8 g/sec, z = 10 cm, R' = 3 ohm, normal polarity.

The graphs in Fig. 5 show U* as a function of z for various values of G at I = 120 A. Clearly, as z increases, U* decreases according to a nonlinear law. At high flow rates (G = 12 g/sec) as z increases the rate of decrease of breakdown voltage $|dU^*/dz|$ at first increases, and then decreases, while at small flow rates (G = 4 g/sec) $|dU^*/dz|$ decreases monotonically with increase in z. It is also clear that as z increases the curves for different flow rates approach each other. A comparison shows that the dependence of U* on z is qualitatively the same for normal and reverse polarity. However, on the investigated range of parameters the value of U* for reverse polarity exceeds that for normal polarity by 10–50%.

The dependence of U* on G is shown in Fig. 6 for I = 160 A. At small z as G increases U* grows rapidly. An examination of the experimental data for various I showed that the effect of I on the change in the absolute value of U* at small z is considerable; however, it diminishes as z increases. Thus, for example, for G = 10 g/sec an increase in current from 80 to 160 A at z = 12.5 cm leads to a decrease in U* from 800 to 530 V, and at z = 5 cm from 3750 to 2270 V.

These characteristic features of the effect of G, I, and z on U* can be explained in terms of the dependence of U* on T_{eff} and δ. By analogy with the generalized Paschen law $U^* = f(p\delta/T)$ for breakdown of the gap between metal

electrodes, U* may be expected to decrease with decrease in the quantity $p\delta/T_{eff}$. As the gas moves along the channel, i.e., with increase in z, it is heated, and ζ increases; consequently, δ decreases.

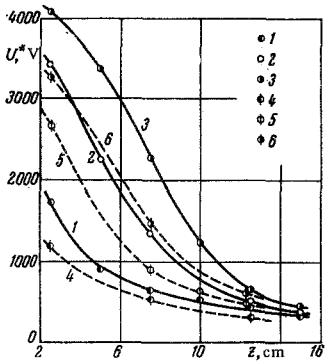

Fig. 5. Variation of the breakdown potential of the arc-wall gap along the channel: for G = = 4 (curves 1, 4), G = 8 (curves 2, 5), G = 12 g/sec (curves 3, 6) at I = 120 A; 1, 2, 3) reverse polarity; 4, 5, 6) normal polarity.

Simultaneously T_{eff} increases, since part of the energy released in the positive column is transferred to the surrounding cold gas. With further increase in z the temperature distribution over the channel cross section tends asymptotically to a limit, i.e., at large z T_{eff} and δ for given I and G tend to definite limits. This process is the more rapid, the smaller G and the larger I. This explains the decrease in U* with increase in z (Fig. 5) and decrease in G (Fig. 6). At small G the gas is heated more rapidly, and U* is close to the limiting value even at small values of z (Fig. 5, G = 4 g/sec), while at large G the gas is heated more slowly, and correspondingly U* approaches the limiting value at large lengths (Fig. 5, G = 12 g/sec). At z = const and I = const as G increases the arc diameter and T_{eff} decrease; consequently, U* increases (Fig. 6). The experiment showed that a decrease in I leads to a similar effect. It is clear from Fig. 6 that for small z (curves 3 and 6) at large G the increase in U* with increase in G slows down. Apparently, this is because in such cases the effect of the arc on the state of the gas in the breakdown gap is small, i.e., T_{eff} is almost equal to the temperature of the cold gas, and in the initial sections at large G the radius ζ depends only weakly on the latter.

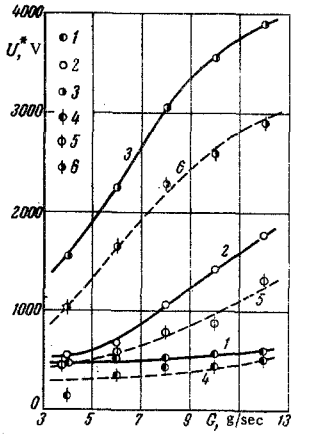

Fig. 6. Breakdown potential of the arc-wall gap as a function of gas flow rate for z = 12.5 (curves 1, 4), z = 7.5 (curves 2, 5), and z = 2.5 cm (curves 3, 6) at I = = 160 A: 1, 2, 3) reverse polarity; 4, 5, 6) normal polarity.

It follows that U* is chiefly determined by the energy balance of the arc and the gas flow. Assuming the constancy of the gas enthalpy at the inlet to the arc chamber, the mean-mass gas enthalpy in section z can be characterized by the quantities

$$k = \frac{I}{G}\int_0^z E_z\,dz \approx \frac{IUz}{aG}, \quad \eta = 1 - Q_z\left(I\int_0^z E_z\,dz\right)^{-1}$$

In first approximation it may be assumed that T_{eff} (or the enthalpy h_{eff} corresponding to that temperature) and δ are determined by these quantities. In [5] the quantity k was taken as h_{eff}. In reality, owing to the sharp nonuniformity of the temperature distribution over the channel cross section the mean-mass enthalpy is much greater than h_{eff}. Accordingly, it should again be emphasized that T_{eff} and h_{eff} are functions only of k and η_z. Considering that in the first approximation η_z is also a function of k, we can construct the simplified relation

$$U^* = f(\beta), \quad \beta = IUz / aG. \tag{3.1}$$

In Fig. 7 the experimental data have been correlated on the basis of (3.1). The more accurate criterial equation for U* [8] has the form:

$$U^* = f\left(\frac{IU}{G}, \frac{G}{d}, pd, \frac{z}{a}, \frac{a}{d}\right). \tag{3.2}$$

In the case in question p = const, d = const, and a = const. Therefore (3.2) may be written as

$$U^* = f\left(\frac{IUz}{aG}, G, z\right). \tag{3.3}$$

A comparison of (3.1) and (3.3) shows that (3.1) must be stratified with respect to G and z. The stratification with respect to z is directly apparent from Fig. 7. The stratification with respect to G at z = const is shown in Fig. 8. As can be seen from Fig. 7, the experimental data presented can be described by Eq. (3.1) correct to ±50%. Therefore generalization of the experimental data in the form (2.1) may be considered useful for estimating the value of U*.

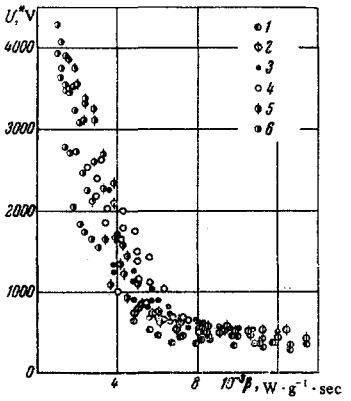

Fig. 7. Breakdown potential as a function of the parameter IUz/aG W·g^{-1}·sec. Points 1, 2, 3, 4, 5, and 6 correspond to the values z = 15, 12.5, 10, 7.5, 5, and 2.5 cm, respectively.

Let us compare the results obtained with the data for the breakdown of air between metal coaxial electrodes. In the latter case the breakdown voltage is determined [9] from the semiempirical formula

$$\ln\left(1+\frac{1}{\gamma}\right) = \frac{A}{B}\frac{T}{T_0}\frac{U^*}{\ln\frac{R}{r'}}\left[\exp\left(-\frac{Bpr_1}{U^*}\frac{T_0}{T}\ln\frac{R}{r_1}\right) - \exp\left(-\frac{BpR}{U^*}\frac{T_0}{T}\ln\frac{R}{r'}\right)\right], \tag{3.4}$$

where T_0 = 300° K.

The results of a calculation based on (3.4) are presented in Fig. 9, where $R - r_1 = \delta$. In the calculations it was assumed that

$$A = 15\frac{1}{\text{cm mmHg}}, \quad B = 365\frac{b}{\text{cm mmHg}}, \quad \gamma = 10^{-2} \quad [10].$$

As seen from (3.4) and the graphs, at R = const, U^*_{min} does not depend on T and p but is determined only by γ. The maximum measured values of γ do not exceed 0.12 [10]; accordingly, the value $\gamma = 0.29$ should be regarded as too high. The value $\gamma = 0.29$ was formally found from the condition of equality of the value of U* calculated from (3.4) and the least experimental value of U* for reverse polarity (plasma as anode) on the investigated range of variation of the parameters.

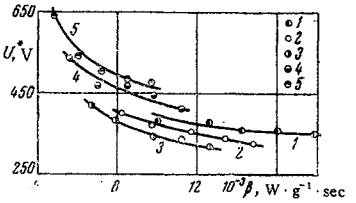

Fig. 8. Breakdown potential as a function of the parameter IUz/aG W·g^{-1}·sec for z = 12.5 cm. Curves 1, 2, 3, 4, and 5 correspond to G = 4, 6, 8, 10, and 12 g/sec.

It should also be emphasized that in the range $\delta = (4-70)10^{-3}$ cm the voltage U* depends rather weakly on γ and decreases with decrease in δ and increase in T. These relations and the data of Fig. 7 have certain properties in common. As noted above, as IUz/aG increases, so does the value of T_{eff}, while δ decreases. Thus, in both cases U* decreases with increase in temperature and decrease in the size of the discharge gap.

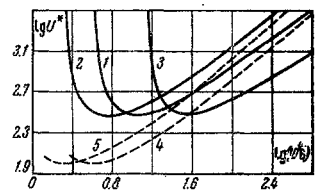

Fig. 9. Theoretical $U^* = f(R - r_1)$ curves for coaxial electrodes at R = 0.5 cm; p = 1 atm abs for curves 1, 3, 4 and p = 2 atm abs for curves 2 and 5; $\gamma = 10^{-2}$ for curves 1, 2, 3 and $\gamma = 0.29$ for curves 4 and 5; T = = 300° K for curves 1, 2, 4, 5 and T = = 1000° K for curve 3.

Clearly, other things being equal, the electric strength of the arc-electrode gap is chiefly determined by the layer of cold gas adjacent to the wall. Since in these experiments the segments were intensively cooled, the temperatures of their inner walls and the adjacent layers of gas did not exceed 1000°K.

The variation of gas pressure along the channel was also slight and remained within the limits 1–2 atm abs. The values of U* from Fig. 7 for given values of the temperature and pressure correspond to a variation of δ in the range $3 \cdot 10^{-3}$–$1.5 \cdot 10^{-1}$ cm (see Fig. 9), large values of δ relating to small z and I and large G. Thus, starting from a comparison of the data of Figs. 7 and 9, we may conclude that if Paschen law $U^* = f(p\delta/T)$ is applicable to the given case, despite the inapplicability of the Townsend-Rogowski theory, then at large z and I and small G the development of the breakdown process begins in a thin layer adjacent to the electrode ($\delta \approx 10^{-1}$–10^{-3} cm). However, it is to be expected that as the current increases during development of the discharge charged particles from ever deeper layers of gas will begin to play an important part in current transport.

The results obtained and the known properties of the semi-self-maintained discharge in the arc-wall gap [11] make it possible to propose the following picture of gas breakdown between a cylindrical column (i.e., $\partial/\partial z = 0$) and the channel wall. The discharge gap can be arbitrarily divided into two regions. The first region borders the column ($\xi < r < r_1$) and contains a relatively large number of electrons and ions. Charged particles penetrate into this region from the arc by diffusion, as well as being created in it directly by photoionization, etc. The axial component of the current density in the first region is negligibly small as compared with the current density in the arc column. The current per unit length of the channel in the radial direction is given by the equations

$$i = 2\pi re\left\{\left(E_r - \frac{v_e H_\varphi}{c}\right) b_e n_e + \left(E_r - \frac{v_i H_\varphi}{c}\right) b_i n_i + D_e \frac{dn_e}{dr} - D_i \frac{dn_i}{dr}\right\} \tag{3.5}$$

$$\frac{1}{r}\frac{d}{dr}(rE_r) = 4\pi e(n_i - n_e) \tag{3.6}$$

At the boundary of the column $r = \zeta$ the value of E_r is small, charge transport depends chiefly on diffusion, and the potential drop U_1 on the interval $\zeta < r < r_1$ is small. As r increases, E_r also increases, and at the boundary of the first region at $r = r_1$ the chief role is played by the motion of charges in the electric field. The second region lies between the first region and the channel wall ($r_1 < r < R$). Here, the gas is relatively cold, $v_e \simeq 0$, $v_i \simeq 0$, current transport depends on E_r, and the current is given by the equation

$$i = 2\pi re E_r (b_i n_i + b_e n_e) \tag{3.7}$$

and Eq. (3.6). If the plasma serves as cathode and $n_i \ll n_e$, Eqs. (3.6) and (3.7) have a solution [9, 12] which at small i and $r_1/R \approx 1$ can be considerably simplified [9] and written in the form:

$$i = \left(U_1 - U_R - r_1 E_1 \ln\frac{R}{r_1}\right) r_1 E_1 b_e \tag{3.8}$$

where $U_1 = U(r_1)$, $E_1 = E_r(r_1)$.

From (3.8) we may conclude that, in spite of the fact that the arc is an almost unlimited emitter of electrons, and γ processes are not required for electron multiplication, at small potential difference ($U_1 - U_k$) the current remains bounded. But, as $U_1 - U_R$ increases, an important new factor appears: at large E_r and i the temperature of the electron gas becomes higher than the temperature of the heavy particles and intense nonequilibrium ionization begins [13]. This ionization is characterized by a specific instability—starting from a certain value of E_r the current density rapidly increases. It may be assumed that in the given case this instability ends in arc breakdown.

The primary electrons produced in the discharge gap by photoionization and the photoemission of the wall may also lead to the development of the above-mentioned instability. Apparently, their role is important when the plasma serves as anode, i.e., when the radial electric field resists the diffusion of electrons into the discharge gap.

It is clear from (3.5) that for positive polarity the signs of E_r and dn_e/dr are the same, while for negative polarity they are different. This explains the difference in the values of U* for positive and negative polarity.

Thus, breakdown of the arc plasma–cold electrode gap has been experimentally investigated. The dependence of the breakdown potential on I, G, and z has been determined, and it has been shown that in the first approximation U* can be represented in the form of a function of the dimensional complex IUz/aG.

REFERENCES

1. H. Tateno and K Saito, "Anodic phenomena in nitrogen plasma, jet.," Japan. J. Appl. Phys., vol. 2, no. 3, 1963.

2. V. Ya. Smolyakov, "Some properties of the arc in a dc plasma generator," PMTF, no. 6, 1963.

3. T. K. Harvey, P. G. Simpkins, and B. D. Adcock, "Instability of arc columns," AIAA Journal, vol. 1, no. 3, 1963.

4. G. Yu. Daumov and M. F. Zhukov, "Some generalizations relating to the study of electric arcs," PMTF [Journal of Applied Mechanics and Technical Physics], no. 2, 1965.

5. V. Ya. Smolyakov, "Criteria of approximate similarity for an arc with self-adjusting length, burning in a plasmatron with vortex gas stabilization," PMTF [Journal of Applied Mechanics and Technical Physics], no. 1, 1967.

6. M. A. Aronov, "Electric strength of the air gap between an open arc column and a wall, "Elektrichestvo, no. 11, 1965.

7. G. Yu. Daumov, Yu. S. Dudnikov, and M. I. Sazonov, "Investigation of a plasma generator with an interelectrode insert," Izv. SO AN SSSR, Ser. tekhn. nauk, 3, no. 10, 1965.

8. G. Yu. Daumov, "A similarity criterion for electrical discharges in gases," PMTF [Journal of Applied Mechanics and Technical Physics], no. 1, 1968.

9. A. von Engel, Ionized Gases [Russian translation], Fizmatgiz, Moscow, 1959.

10. Meek and Craggs, Electrical Breakdown of Gases [Russian translation], IL, Moscow, 1960.

11. G. Yu. Daumov and M. I. Sazonov, "Electric field strength in a stabilized vortex arc," PMTF [Journal of Applied Mechanics and Technical Physics], no. 4, 1967.

12. N. A. Kaptsov, Electrical Phenomena in Gases and a Vacuum [in Russian], Gostekhizdat, Moscow-Leningrad, 1947.

13. J. L. Kerrebrok, "Nonequilibrium ionization due to electron heating I: Theory," AIAA Journal, vol. 2, no. 6, 1964.

21 October 1968

Novosibirsk